

-11
DOE/BC/14893-11
PRRC 96-03

Quarterly Technical Report

INTEGRATION OF ADVANCED GEOSCIENCE AND ENGINEERING TECHNIQUES TO
QUANTIFY INTERWELL HETEROGENEITY

DOE Contract No. DE-AC22-93BC14893

RECEIVED
MAR 11 1996
OSTI

New Mexico Petroleum Recovery Research Center
New Mexico Institute of Mining and Technology
Socorro, NM 87801
(505) 835-5142

Contract Date:

September 29, 1993

Anticipated Completion Date:

September 30, 1996

DOE Award for FY 1995:

\$250,896

Program Manager:

F. David Martin

Principal Investigators:

Jill S. Buckley

William W. Weiss

Ahmed Ouenes

Contracting Officer's
Representative:

Robert E. Lemmon

Bartlesville Project Office

Reporting Period:

October 1, 1995 - December 31, 1995

US/DOE Patent Clearance is not required prior to the publication of this document.

DISCLAIMER

This report was prepared as an account of work sponsored by an agency of the United States Government. Neither the United States Government nor any agency thereof, nor any of their employees, makes any warranty, express or implied, or assumes any legal liability or responsibility for the accuracy, completeness, or usefulness of any information, apparatus, product, or process disclosed, or represents that its use would not infringe privately owned rights. Reference herein to any specific commercial product, process, or service by trade name, trademark, manufacturer, or otherwise does not necessarily constitute or imply its endorsement, recommendation, or favoring by the United States Government or any agency thereof. The views and opinions of authors expressed herein do not necessarily state or reflect those of the United States Government or any agency thereof.

DISTRIBUTION OF THIS DOCUMENT IS UNLIMITED

JR

MASTER

OBJECTIVE

The objective of this project is to integrate advanced geoscience and reservoir engineering concepts with the goal of quantifying the dynamics of fluid-rock and fluid-fluid interactions as they relate to reservoir architecture and lithologic characterization. This interdisciplinary effort will integrate geological and geophysical data with engineering and petrophysical results through reservoir simulation. Subcontractors from Stanford University and the University of Texas at Austin (UT) are collaborating on the project. Dr. Jerry Harris, Associate Professor in the Department of Geophysics at Stanford, is supervising the geophysical research. Dr. Gary Pope, Director of the Center for Petroleum and Geosystems Engineering at UT, is supervising the hydrologic and tracer research. Several members of the PRRC staff are participating in the development of improved reservoir description by integration of the field and laboratory data, as well as in the development of quantitative reservoir models to aid performance predictions.

SUMMARY OF TECHNICAL PROGRESS

GEOLOGIC STUDIES

Core Analysis

During the previous quarter, core from Sulimar Queen Well 1-16 was analyzed in detail: core description was made on an inch by inch basis; permeabilities were measured every half inch; and grain size analysis was completed at 6 in. intervals.

The detailed core description shows two major shallowing upward sequences (Fig. 1). The Shattuck member in this part of the Sulimar Queen Field was deposited in a shallow aqueous environment, probably a tidal environment as evidenced by the presence of thin shale laminations, flaser bedding, and bioturbation and fine grain size. The distribution of individual lithological units are controlled by minor changes in water depth and energy conditions.

Permeability measurements made using a minipermeameter demonstrate that permeability is closely tied to minor changes in the lithology (Fig. 2). Based on permeability distribution, the Shattuck can be divided into two parts: the upper (from 1994 - 2004 ft) high permeability zone and the lower (from 2005 - 2015 ft) low permeability zone. The upper high permeability zone is the more heterogeneous zone (Fig. 2). Comparison of the permeability curve in Fig. 2 with the core gamma ray curve measured by Core Laboratories (Fig. 3) shows that the high permeability zones coincide nicely with the high gamma ray zones. This is probably because, in the Queen Formation, high gamma ray readouts are caused by large amounts of potassium feldspar, which is most common in the higher permeability, sand-sized fraction of the formation. This relationship between gamma ray curves and porosity and/or permeability could prove useful for in neural networks designed to create synthetic porosity/permeability curves for the other wells within the Sulimar Field.

For permeability distribution, 44 samples were collected from the core for grain size analysis, using the Folk method.¹ Grain size analysis shows that in Well 1-16, the Shattuck Member of the Queen Formation consists of very fine grained silty and clayey sandstone; its variability appears to exert the major controls on sample permeability (Fig. 4). As the amount of sand-sized material increases, so does permeability. Figures 4(a), (b), and (c) show the actual correlation between permeability and different textural elements. There is an overall decrease in permeability as amounts of clay and cement decreases; however, none of the correlations is very high.

Identifying depositional environment and distribution of individual lithological units, the data obtained will be helpful in developing correlations between porosity and permeability, after porosity at the

same scale is obtained. It will also improve the utility of old logs for porosity calculations.

SWWTT DESIGN FOR SULIMAR QUEEN FIELD (UNIVERSITY OF TEXAS AT AUSTIN)

The preliminary design for the Single Well Wettability Tracer Test (SWWTT) for the Sulimar Queen Field was reported in our last annual report. Ethyl formate and propyl formate were the reacting tracers used in our design. The simulation results reported were for a weakly water wet media. The injection rate of 15.5 bbls/day and the production rate of 8 bbls/day were used. We conducted numerous simulations to investigate the significance of reservoir and fluid properties on our preliminary design.

Tracer Properties

We first performed sensitivity simulations to investigate the effect of tracer properties such as partition coefficients and reaction rates on the design factors such as the duration of tracer injection and tracer concentrations. The water tracers used are reacting ethyl formate with the product tracer of ethanol and methanol as a nonreacting conservative tracer. The tracers used with the oil slug are reacting propyl formate tracer with the product tracer of normal propyl alcohol. The nonpartitioning nonreacting oil tracer used is octanol. The limited published data available on the partition coefficient and the hydrolysis rate for these tracers with different oils show a 50% deviation on the hydrolysis rate and a 10% deviation for the partition coefficients. We included these levels of uncertainty in our simulations. The peak tracer concentrations were greatly affected but within the range that no change was required in our tracer concentration or tracer slug size from those used in the earlier design.

Reservoir Properties

The next sensitivity parameter was the ratio of vertical to horizontal permeability. This ratio was 0.1 in our preliminary design. We performed simulations for the two limiting values of no crossflow ($k_z/k_x = 0$) and with complete cross flow ($k_z/k_x = 1$). The results were not sensitive to the magnitude of the crossflow.

The effect of reservoir wettability was also studied by incorporating different relative permeability and capillary pressure curves for weakly water wet (WWW), weakly oil wet (WOW), and moderately oil wet (MOW) wettability conditions. Both residual water and oil saturations, and endpoint relative permeabilities were shifted in the Corey relative permeability function for different wettability conditions consistent with the trend found in the literature. The WWW and WOW results were very similar. The differences observed for MOW were not significant enough to affect the basic test design.

Physical Properties

To examine the effect of relative permeability and capillary pressure functions different than the Corey function, we used the capillary pressure function of van Genuchten,² and the relative permeability functions developed by Parker *et al.*³ The main difference between these results and those using Corey functions was in the computed bottomhole pressure.

Test Design

We also studied the effect of different slug injections in the design. For example, the necessity and impact of injection of water or oil slug buffers during the test on the extent of the information we obtain from the test. We are in the process of simulating the thiocyanate tracer test performed in Sulimar Queen field in December 1995.

FIELD OPERATIONS

During the last quarter of 1995, Well 1-16 was the site of a nonreactive tracer test. The purpose of this test was to gain field experience for the in-situ wettability tracer test scheduled for the first quarter of 1996. Approximately five pounds (4.87 lb) of ammonium thiocyanate (CNS) were dissolved in 100 bbl of produced water (~305,000 ppm TDS). The injection concentration of the tracer in the 100 bbl plastic tank set beside Well 1-16 was 139 mg/l prior to injection.

Between October 20, 1995 and November 22, 1995, hydrostatic pressure (~266 psi) was used to drain 90 bbl of the 139 mg/l CNS solution into the well. The injection rate increased during the 32-day period as illustrated in Fig. 5.

Twenty hours prior to opening the Well to tracer injection, a wireline bottomhole pressure bomb was placed in Well 1-3, located 270 ft to the west of Well 1-16. The pressure response at Well 1-3 to the gravity injection at Well 1-16 is shown in Fig. 6.

In 650 hrs, 90 bbl of tracer had drained from the tank. When the tank emptied 75 hours later and as the fluid level dropped in Well 1-16, the pressure decreased about 1 psi at the observation well. Finally, on November 25, the bottomhole pressure bomb was replaced and the pressure changes that occurred at Well 1-3 during the time the tracer was pumped from Well 1-16 were recorded.

Well 1-16 was put on production on November 27 to pump out the nonreactive tracer. Initially, the fluid was produced through a half-inch macaroni string tied to the tubing. The small OD tubing was intended to minimize mixing effects as the tracer traveled to the surface. However, the macaroni string failed after four hours and was removed. The tracer was then produced through two-inch tubing into the 100 bbl tracer storage tank. The tank was gauged when samples were collected, which was approximately at one-barrel intervals. The tracer concentration was determined at the HOWE laboratory facility on the New Mexico Junior College campus in Hobbs, NM. These results are illustrated in Fig. 7 and in Fig. 8. Sampling of the produced fluid from Well 1-16 continues. An analysis of the tracer concentrations and the pressure response at Well 1-3 will be reported in the next quarterly report.

RESERVOIR MODELING

The characterization effort is currently focused on building reservoir models which honor the existing and derived data. The two major steps involved in this approach consists of 1) identifying the major lithofacies classes and, more importantly, their spatial distribution, and 2) estimating the petrogeological properties within each class of lithofacies. In the first step, geology and log data were used to locate the two major geologic zones which affect rock properties. These two major zones were deposited in different environments. One was deposited in the eolian (probably dunes) environment and the other in a tidal environment. The next step consists of estimating the porosity, permeability, and initial water saturation in each zone. As a means for better understanding the spatial distribution of reservoir properties, outcrop data are analyzed.

Geostatistics of the Bonetank Draw Formation Outcrops

To facilitate and improve the quality of input data in the numerical simulation of the Sulimar Queen reservoir, it is important to understand the geological characteristics of the formation. This understanding can be facilitated by outcrop studies. One of the important Queen outcrops is the Bonetank Draw. The

outcrop is designated as #7 on the surface map (Fig. 9). The general structure of the outcrop is shown in Fig.10.

As seen in Fig. 10, the bonetank outcrops in three distinct sections designated as 1, 2, and 3. Careful sampling was done along these outcrops at regularly spaced intervals. The sampling included the measurement of permeability using a portable permeameter as well as extracting core plugs of 1 inch diameter for laboratory measurements. The total number of samples taken at the site is 537.

To determine the general spatial distribution of permeability measurements along the outcrops, the data was subjected to some fundamental geostatistical analysis. The analysis entailed plotting the histograms of the distributions. First the histograms were plotted for the individual outcrops 1, 2 and 3. The distributions were distinctly skewed to the left with a long tail. To visualize the distributions better and to understand their nature, the original histograms were log-normalized. This normalization routine appeared to provide a better distribution of data as shown in Figs. 11(a), 12(a), and 13(a). Along with individual outcrops, the overall permeability distributions in Bonetank as a whole unit were studied. Figure 14 clearly indicates two distinct distributions; permeability bins approximately from 0.00 to 1.20 and 1.50 to 2.39. This split-up of permeability distributions is also evident in Bonetank 2 and Bonetank 3 as shown in Figs. 12(a) and 13(a). Bonetank 1, on the other hand, displays a unimodal log-normal distribution. These results could be significant from a reservoir simulation perspective.

The histograms of the individual outcrops give an insight to the distribution of permeabilities in the Bonetank Draw in a general sense. Variogram analysis is required to see how far the permeability distributions are correlated. The results of the variogram analysis are shown in Figs. 11(b), 12(b), and 13(b). A spherical model is fit for all the data to maintain consistency of comparison. Bonetank 1 displays a relatively strong correlation of the permeability values spatially. It has a range of approximately 20 lags and a sill of 3400. A relatively strong correlation is expected because the data for Bonetank 1 indicates a single log-normal distribution in the histogram. Bonetank 2 displays a strong correlation of the permeability values up to its range which is about 20 lags. However, past 20 lags, the data indicates a significant scatter. The scatter is attributed to the second distribution indicated in the corresponding histogram for Bonetank 2. A very weak correlation is evident in Bonetank 2 variogram analysis. These results suggest dividing the Queen formation into two sections for simulation purposes.

Based on this valuable information concerning the distribution of permeability, a more detailed modeling process using log data can be initiated.

A New Approach for Modeling the Sulimar Queen

Using the neural network described in the last annual report, the porosity profile at the producing wells was obtained and formed the basis for reservoir modeling. A review of the porosity profiles, core data, and outcrop information led to the identification of three major vertical zones in the Sulimar Queen reservoir. The upper part of the reservoir consists of sands characterized with good porosity and permeability. The middle part is represented by a thin layer or a combination of thin shaly sands characterized by low permeability and reasonable porosity. The lower part of the reservoir is made of low permeability and porosity sands.

The use of crosswell tomography between Wells 1-3 and 1-16 provides valuable information on the sedimentation process that led to the formation of the three parts constituting the Sulimar Queen. Furthermore, the choice of the two wells location appears optimal for understanding the sedimentation process, where the separation between eolian and tidal environments lies between the two wells. Thus, Well 1-16 provides valuable information on wet sands (tidal), and Well 1-3 on dune sands.

Additionally, crosswell tomography is currently being used to estimate interwell porosity, using a new interpretation technique. The results of this new approach will be described in future reports. Based on the qualitative and quantitative information provided by crosswell tomography, outcrop studies, and reservoir engineering data, it appears that only the upper part of the Sulimar Queen produced significant oil.

Modeling the Sulimar Queen producing interval starts by averaging the porosity profile obtained at each well using the neural network. Using geostatistics and the average porosity at each well, various models of porosity maps will be generated for the Sulimar Queen. Since permeability for all wells is not available at either core or at well test scale, the strategy used in modeling permeability is to assume the existence of a correlation between porosity and permeability for each lithofacies.

$$k = 10^{A\phi - B} \quad (1)$$

The porosity and permeability used in Eq. 1 refers to a reservoir simulation gridblock. The coefficients A and B used in the correlation are unknown and will be estimated using a production history matching procedure. In other words, a reservoir simulator will use a trial and error procedure to estimate the unknown coefficients A and B that will lead to the best match of the past reservoir performance. This strategy for estimating permeability distribution relies on a single porosity map which needs to be selected from a set of realizations obtained with different geostatistical methods.

Reservoir simulation will be used to select the best porosity map estimated with geostatistical methods. Using the core permeability and porosity data available at well 1-16, a correlation was derived (Fig. 15). The resulting correlation will be used to derive a permeability map for the forward reservoir simulator. Hence, each porosity map corresponds to a permeability map obtained with the core scale derived correlation. Testing all the geostatistical generated maps with a black oil simulator leads to the selection of the best porosity map. The selection criteria is based on the mismatch between actual and simulated reservoir performance. Finding the best porosity map leads to the estimation of the optimum coefficients A and B for the porosity-permeability correlation. The results of this methodology will be described with more details in future reports.

REFERENCES

1. Folk, R.L.: *Petrology of Sedimentary Rocks*, Hemphill Publishing Company, 1980.
2. Van Genuchten, M.T.: "A Closed-form Equation for Predicting the Hydraulic Conductivity of Unsaturated Soils," *Soil Sci. Soc. Am. J.*, **44**, 892-989, 1980.
3. Parker, J.C., Lenhard, R.J., and Kuppusamy, T.: "A Parametric Model for Constitutive Properties Governing Multiphase Flow in Porous Media," *Water Resources Research*, **23** (4), 618-624, 1987.

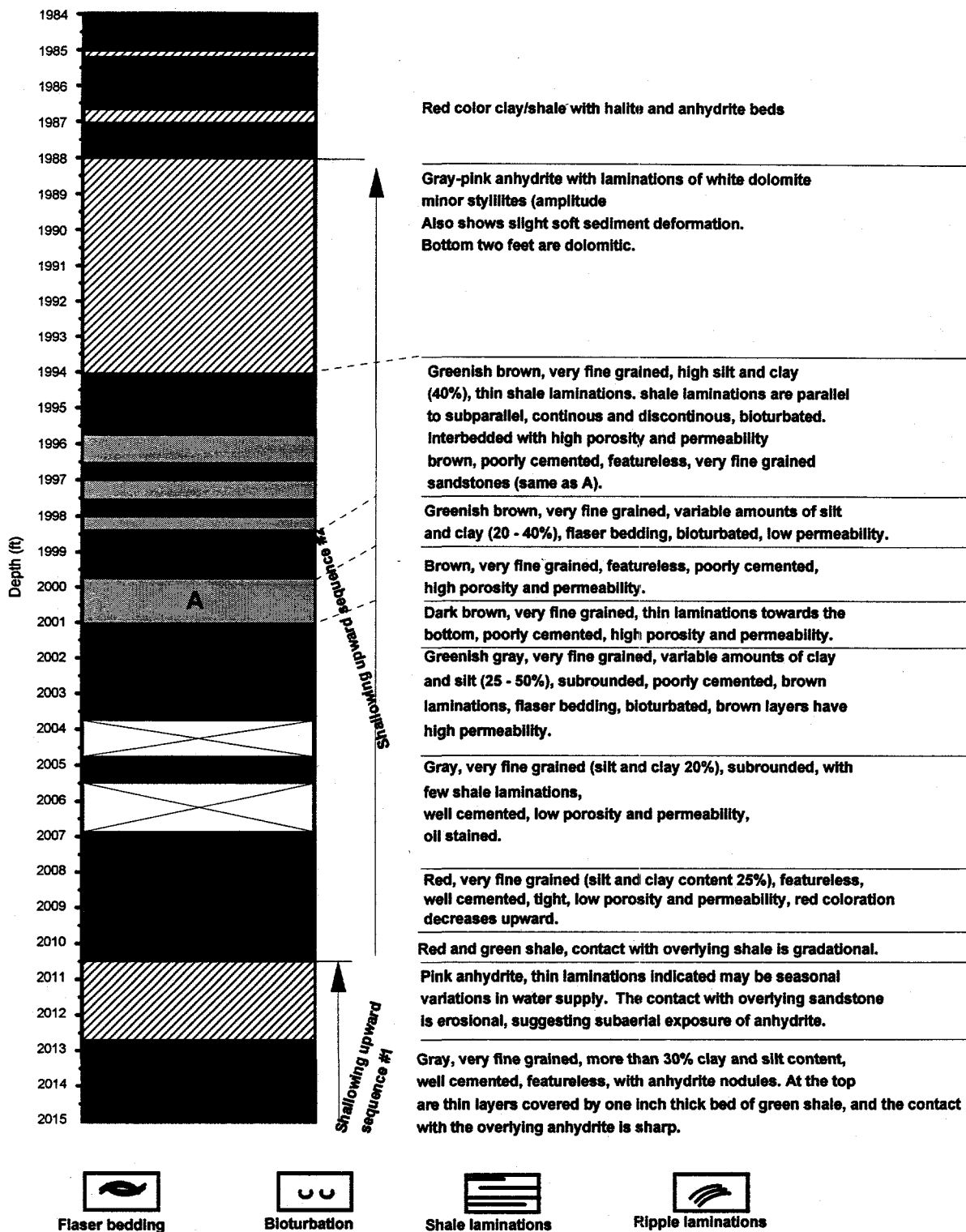


Fig. 1 Core description from well 1-16, Sulimar Queen Field, Chaves County, New Mexico.

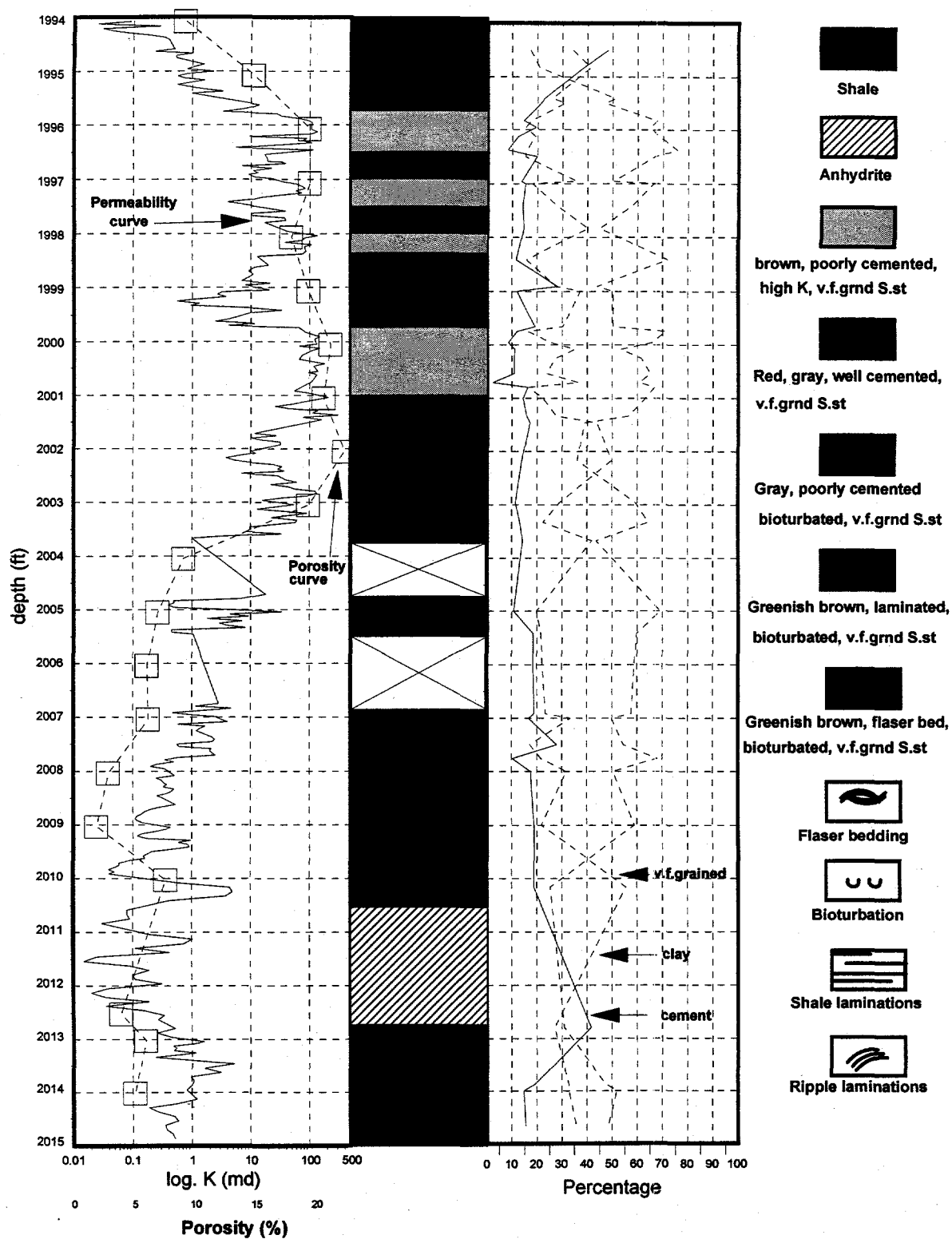


Fig. 2 Summary of core description, and distribution of porosity, permeability, grain size, and cement for core from Well 1-16, Sulimar Queen Field, Chaves County, New Mexico.

Sulimar Queen Unit

1-16

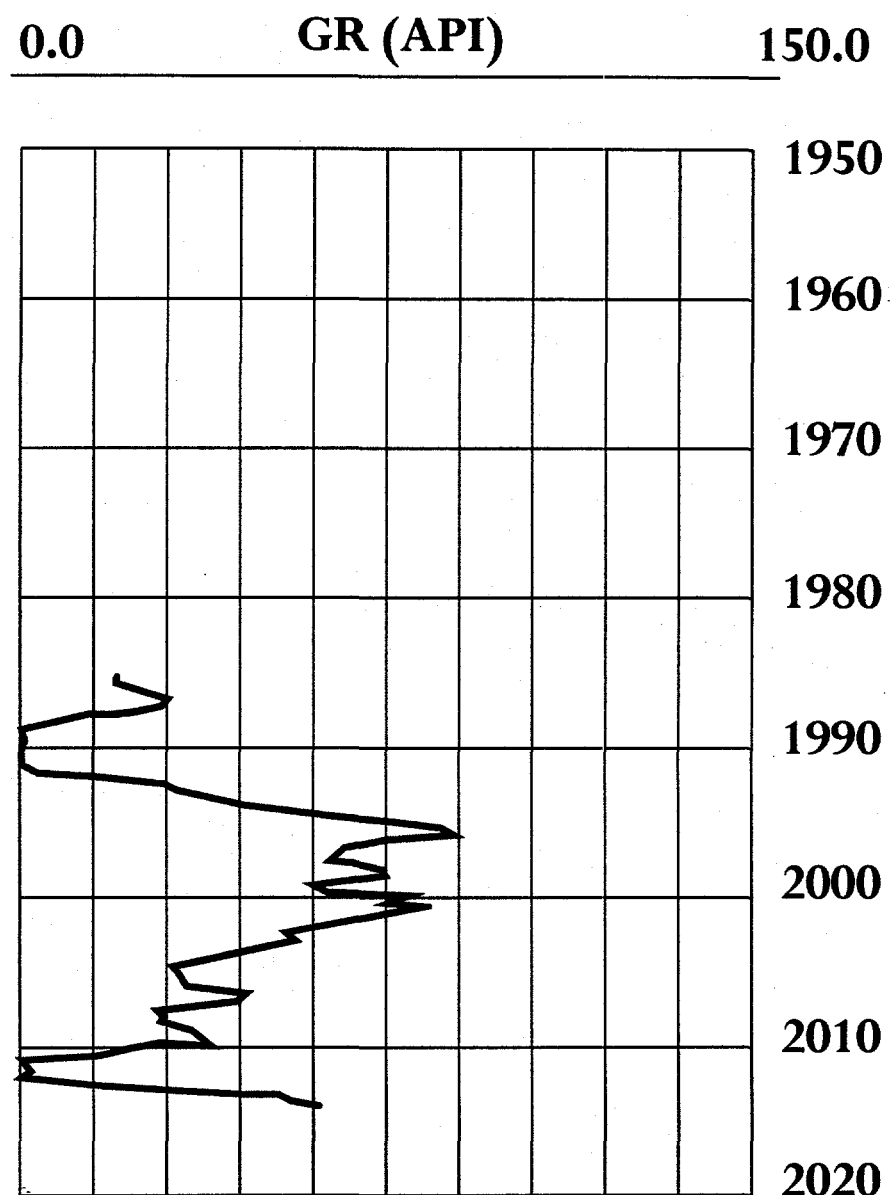


Fig. 3 Gamma ray curve for core 1-16, measured by Core Laboratories.

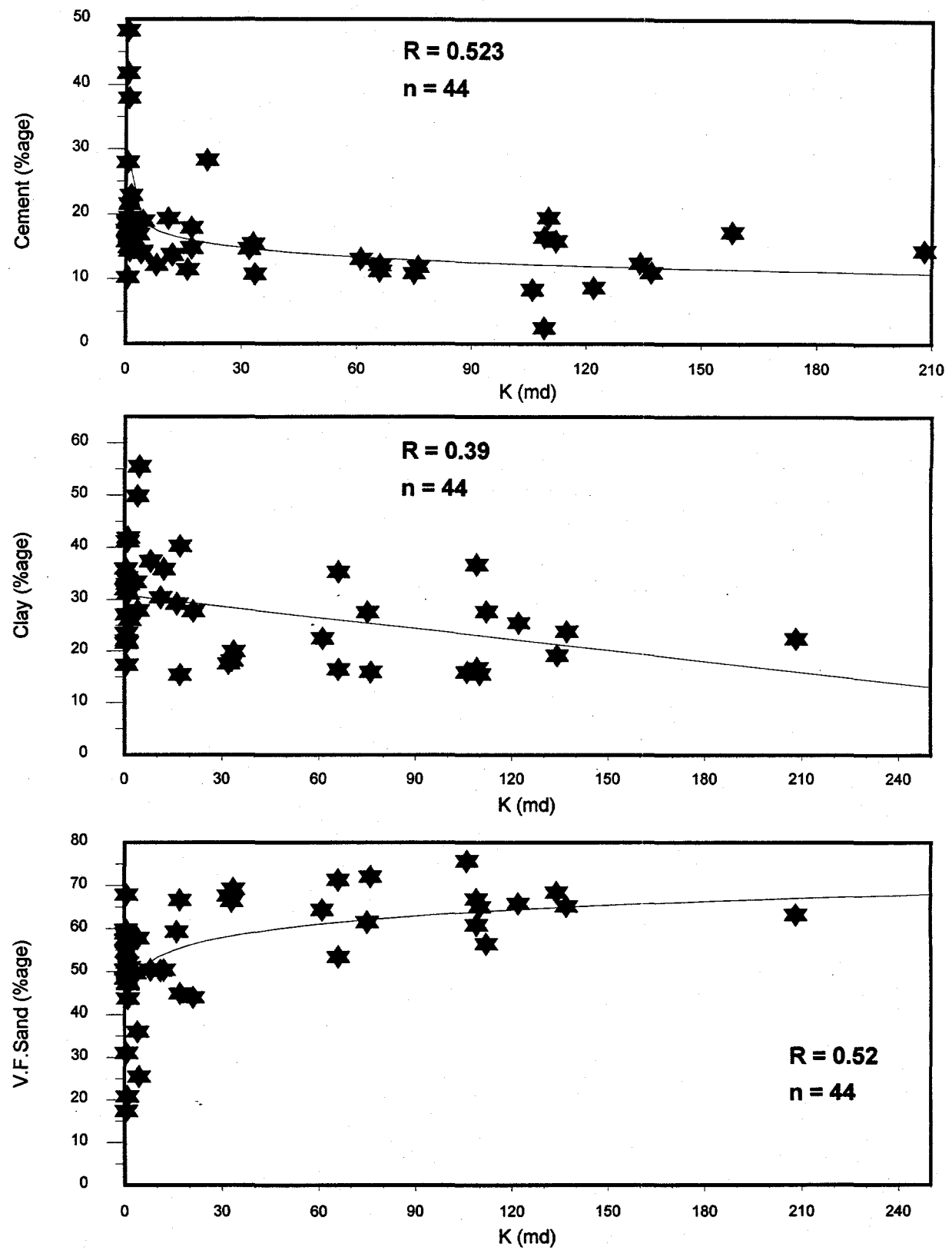


Fig. 4 Plots showing relationship of permeability with cement, clay, and sand percentages in core from well 1-16, Sulimar Queen Field, Chaves Co., New Mexico.

Well 1-16 Tracer Injection

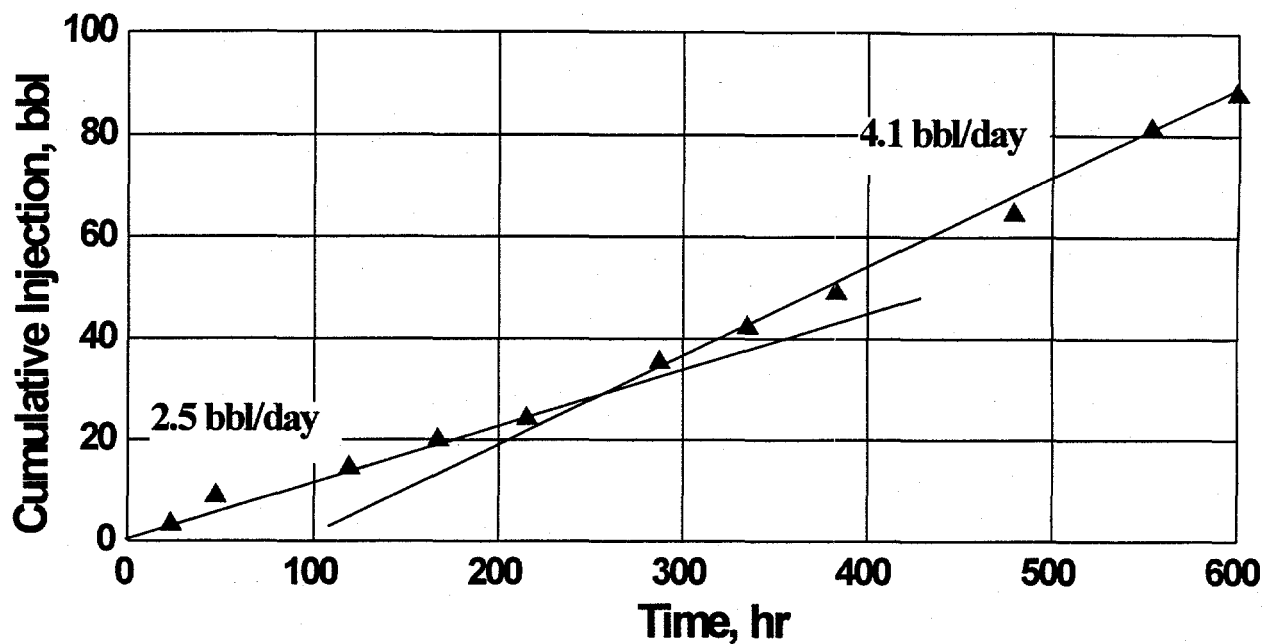


Fig. 5 Tracer Injection.

Well 1-3 Pressure Response Oct. 20 to Nov. 22, 1995

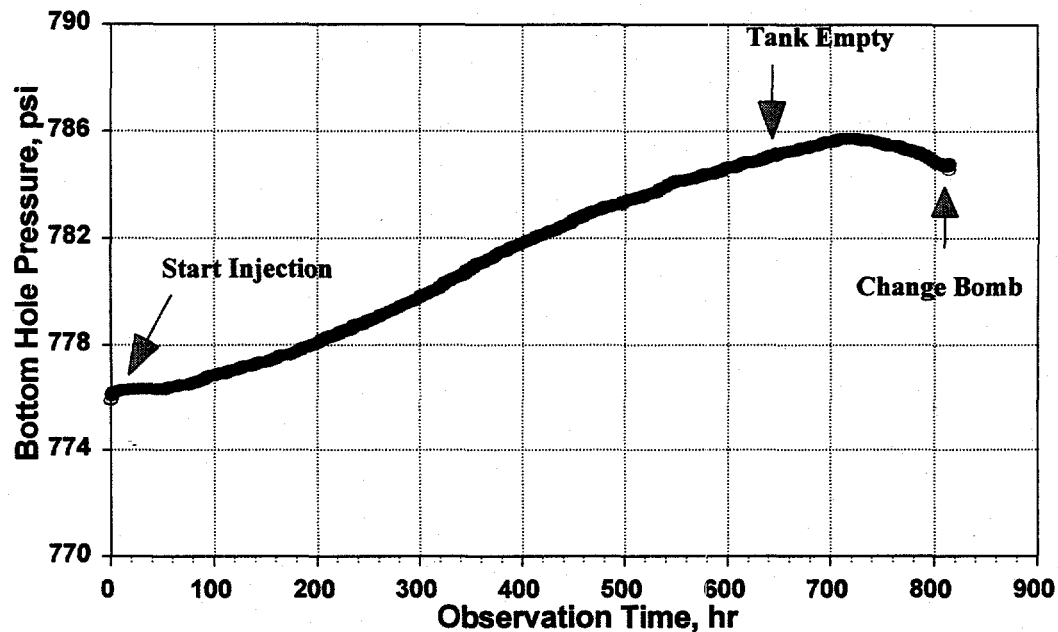


Fig. 6 Pressure response 270 ft from Well 1-16.

Well 1-16 Tracer Injection

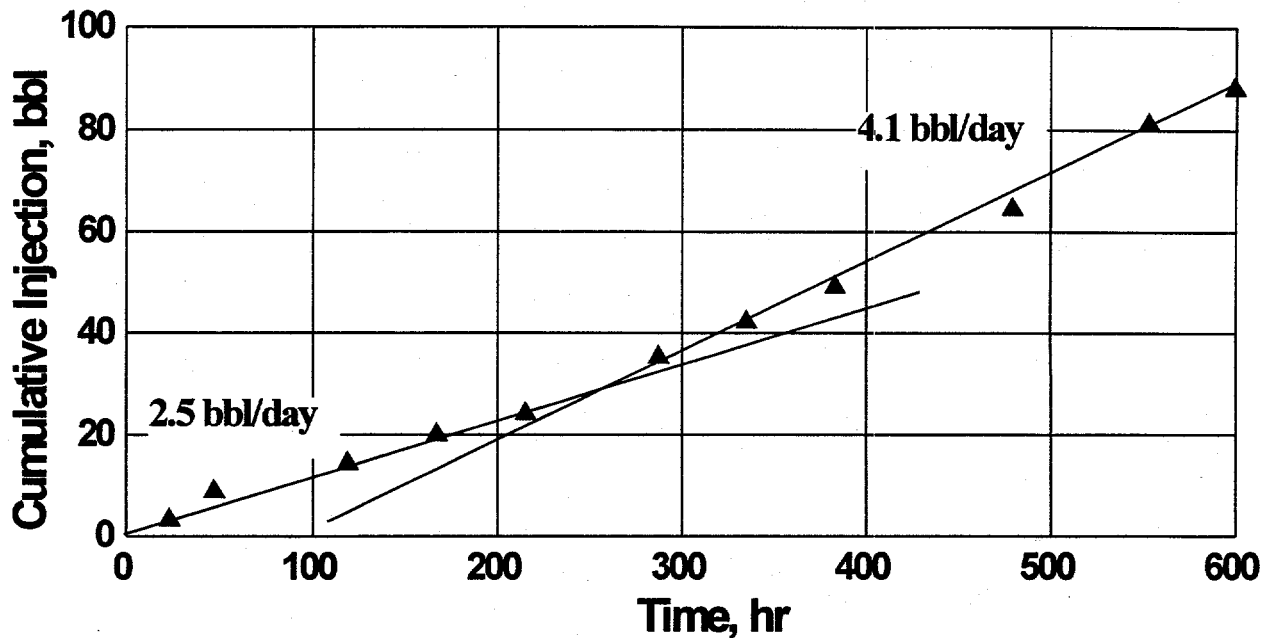


Fig. 7 Tracer as function of production time.

Nov. 27 - Dec. 5, 1995 Tracer Profile

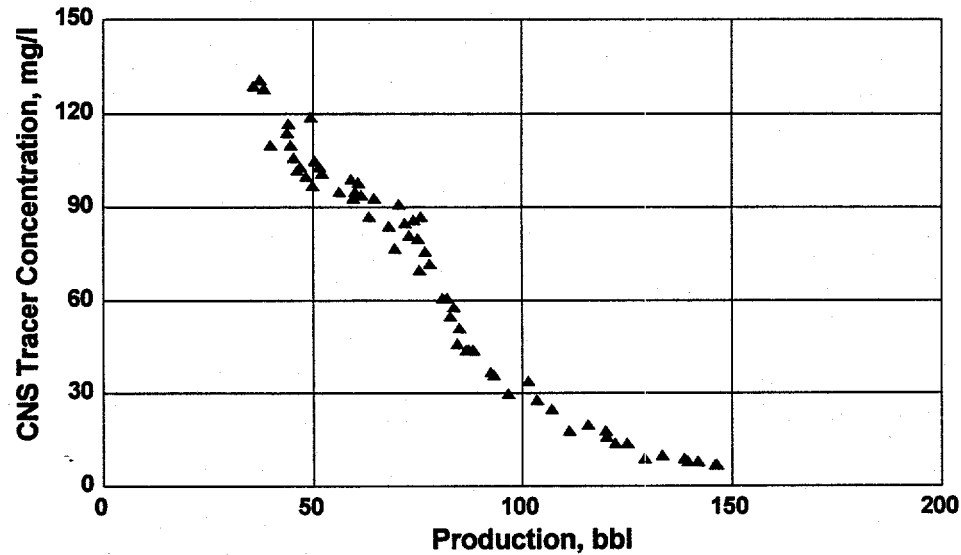
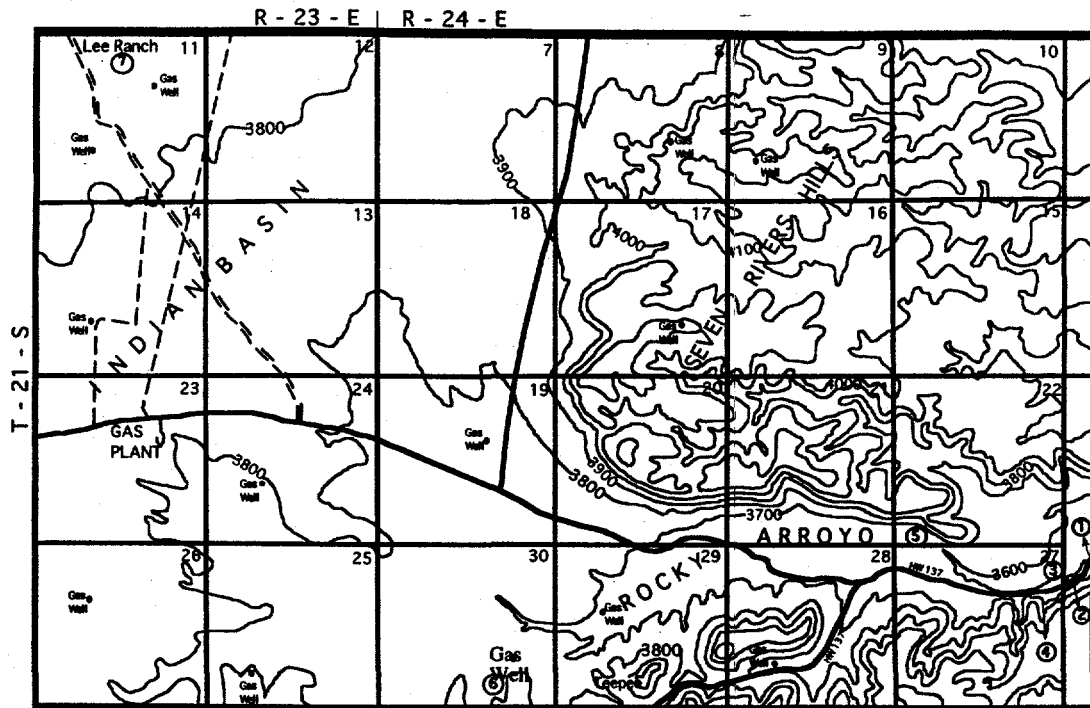


Fig. 8 Tracer as function of cumulative production.



Bonetank 1

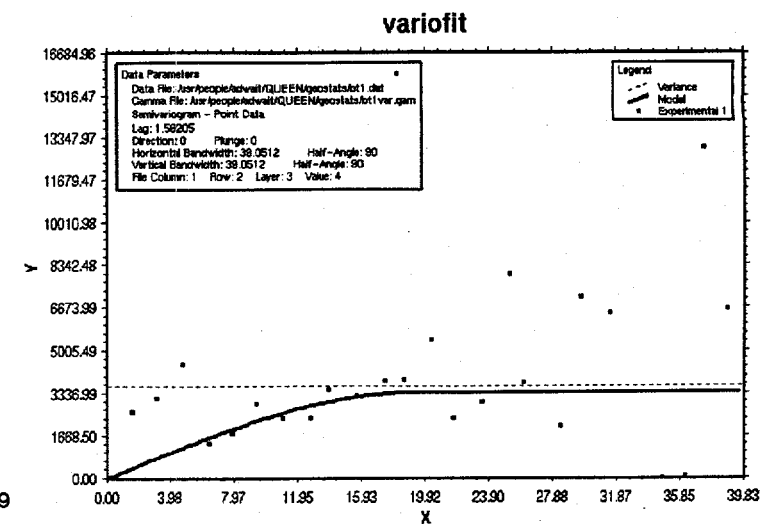
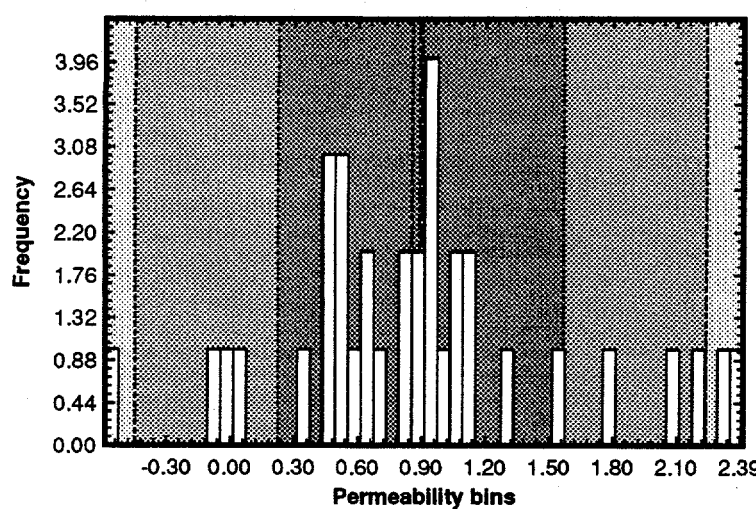


Fig. 11 Log-normalized histogram and variogram analysis for Bonetank 1.

Bonetank 2

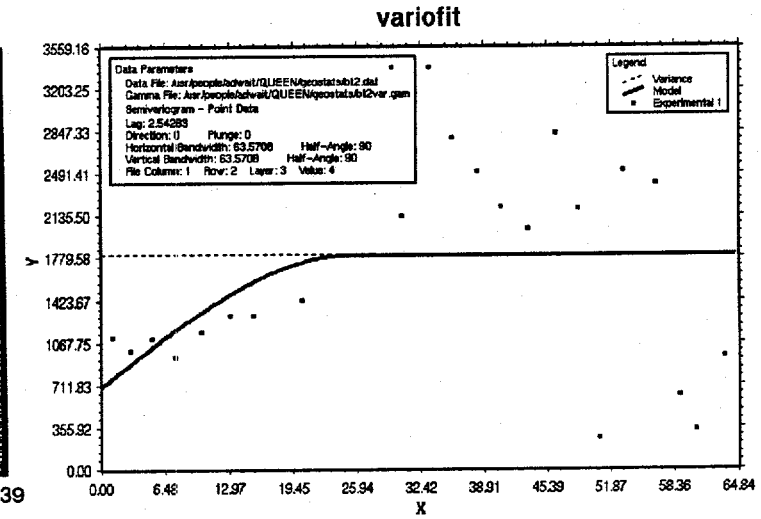
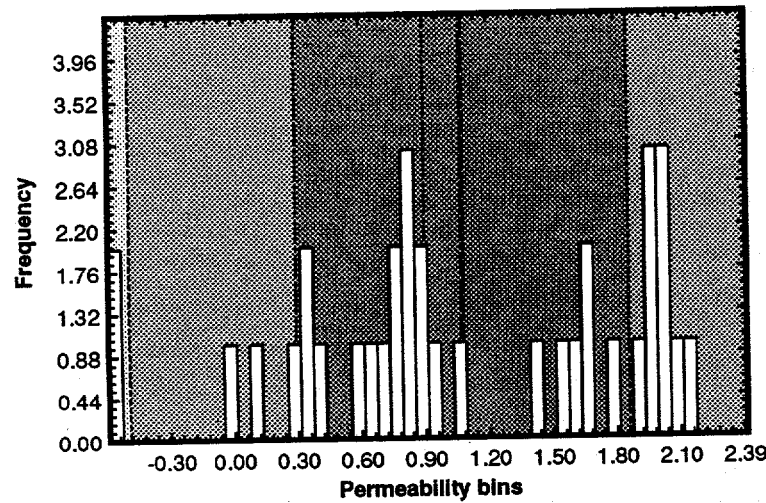


Fig. 12 Log-normalized histogram and variogram analysis for Bonetank 2.

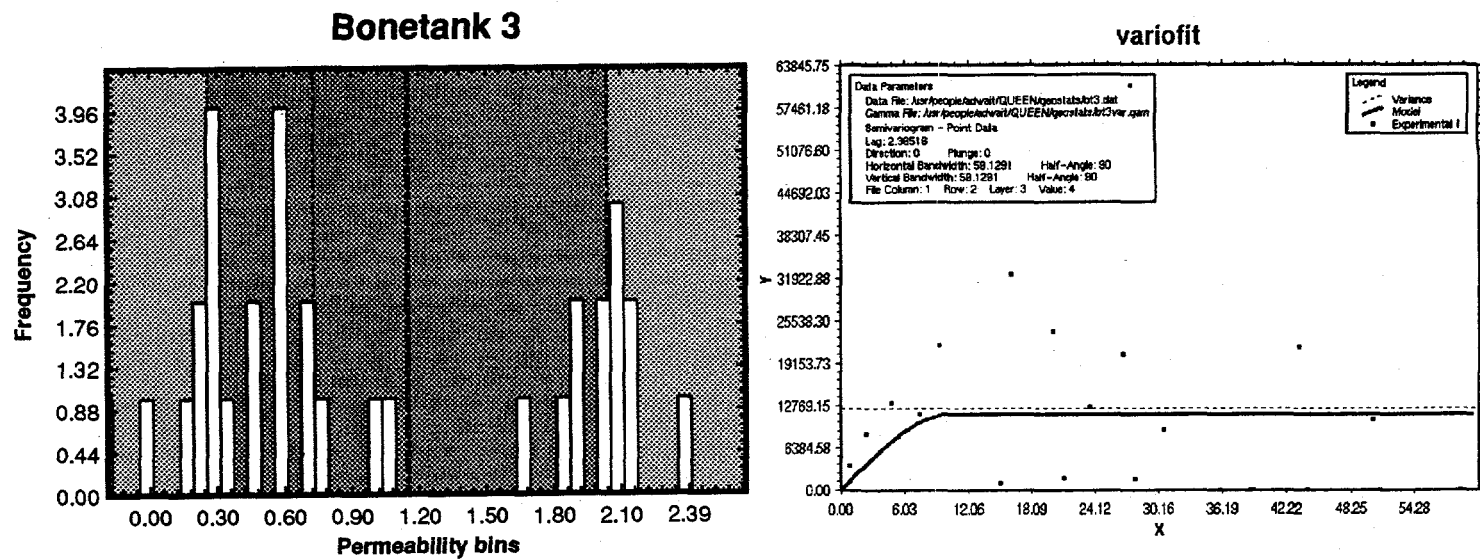


Fig. 13 Log-normalized histogram and variogram analysis for Bonetank 3.

Bonetank

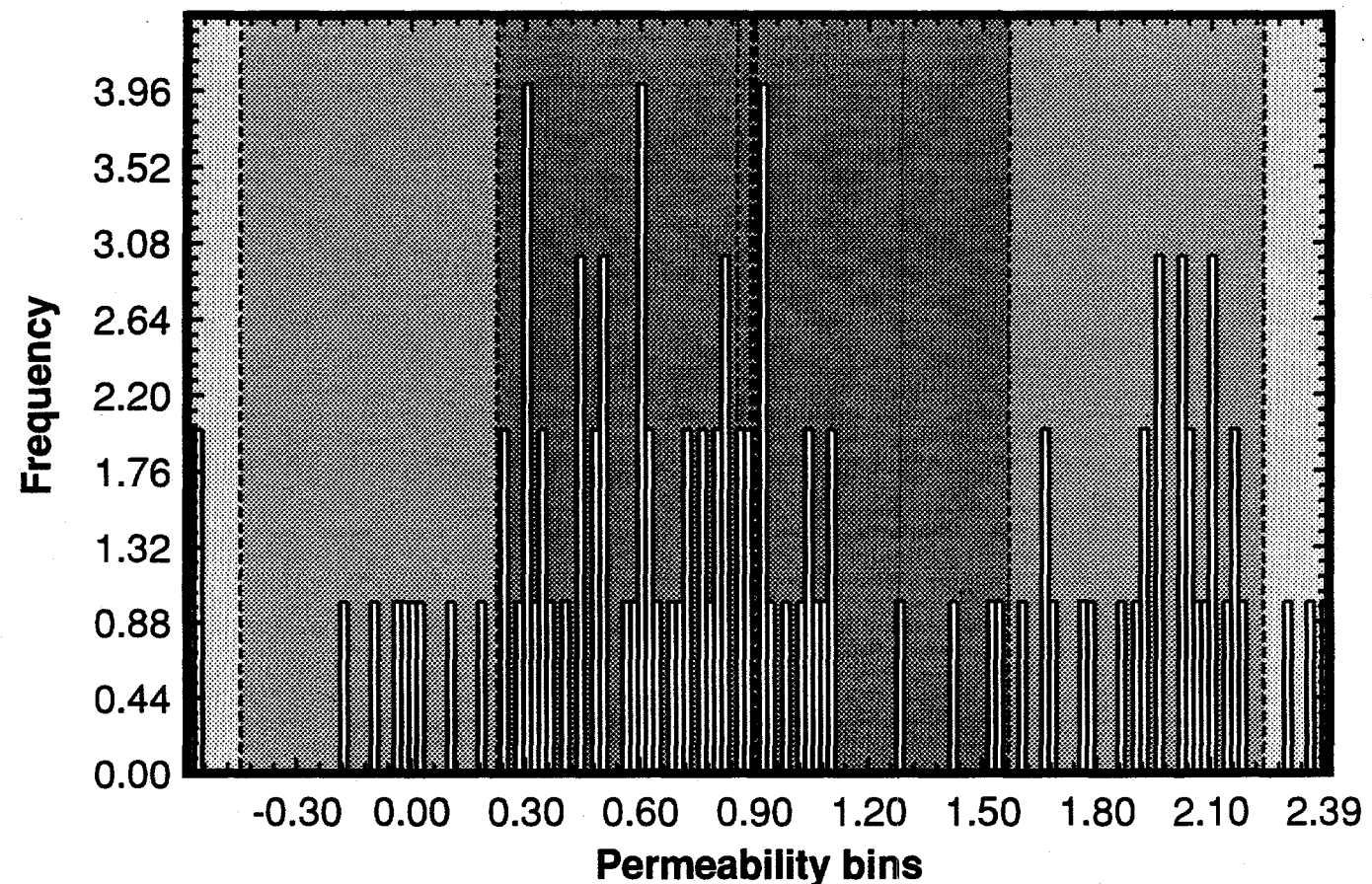


Fig. 14 Log-normalized histogram and variogram analysis for complete Bonetank data.

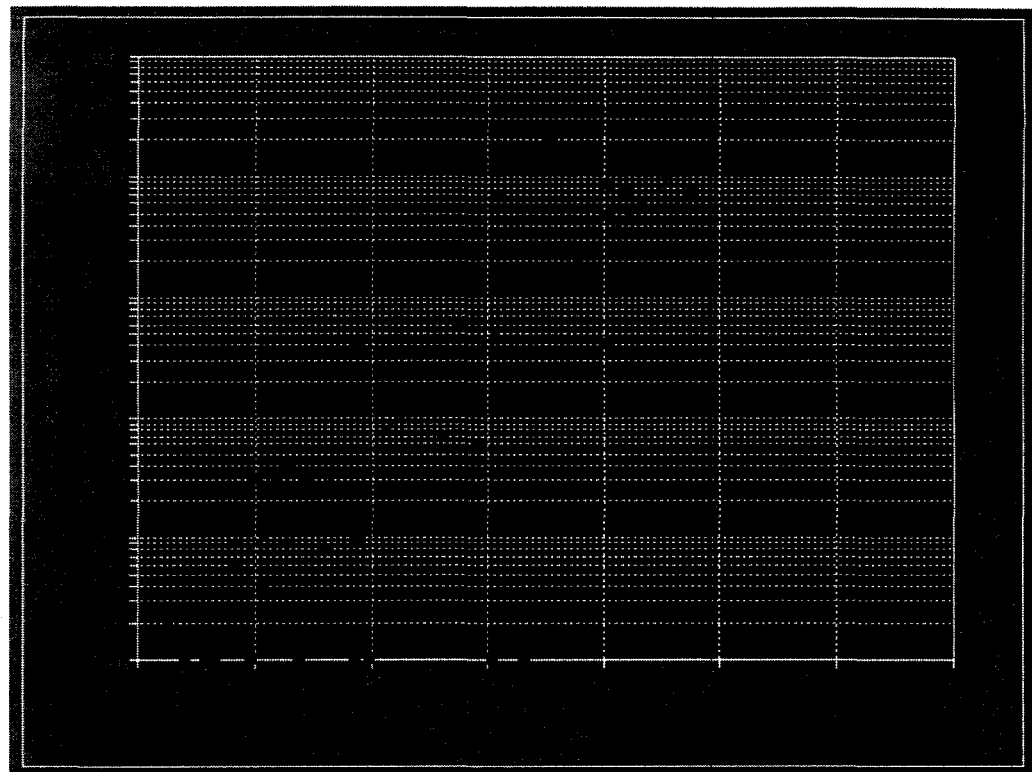


Fig. 15 Core scale porosity-permeability correlation.